

1 **Virus-derived DNA forms mediate the persistent infection of tick cells by**  
2 **Hazara virus and Crimean-Congo hemorrhagic fever virus**

3 Maria Vittoria Salvati<sup>a</sup>, Claudio Salaris<sup>a</sup>, Vanessa Monteil<sup>b,c</sup>, Claudia Del Vecchio<sup>a</sup>, Giorgio Palù<sup>a</sup>,  
4 Cristina Parolin<sup>a</sup>, Arianna Calistri<sup>a</sup>, Lesley Bell-Sakyi<sup>d</sup>, Ali Mirazimi<sup>b,c,e\*</sup>, Cristiano Salata<sup>a\*</sup>

5 <sup>a</sup>Department of Molecular Medicine, University of Padova, Via Gabelli, 63, IT-35121 Padova, Italy

6 <sup>b</sup>Department of Microbiology, Public Health Agency of Sweden, Nobels Väg 18, SE-171 82 Solna,  
7 Sweden

8 <sup>c</sup>Department of Laboratory Medicine, Karolinska University Hospital and KI, SE-14186 Huddinge  
9 Stockholm, Sweden

10 <sup>d</sup>Department of Infection Biology and Microbiomes, Institute of Infection, Veterinary and  
11 Ecological Sciences, University of Liverpool, Liverpool Science Park IC2, 146 Brownlow Hill,  
12 Liverpool L3 5RF, United Kingdom.

13 <sup>e</sup>National Veterinary Institute, SE-756 51, Uppsala, Sweden

14 \*Corresponding authors:

15 Cristiano Salata, Department of Molecular Medicine, University of Padova, Via Gabelli, 63, IT-  
16 35121 Padova, Italy. Phone: +390498272364; e-mail: [cristiano.salata@unipd.it](mailto:cristiano.salata@unipd.it)

17 Ali Mirazimi, Department of Laboratory Medicine, Karolinska University Hospital and KI, SE-  
18 14186 Huddinge Stockholm, Sweden. e-mail: [ali.mirazimi@ki.se](mailto:ali.mirazimi@ki.se)

19 **Running title:** role of vDNAs in tick cell infection

20 **Abstract:** 230 words

21 **Text:** 4963 words

22 **Figures and tables:** 8

23

24

25

26 **ABSTRACT**

27 Crimean-Congo hemorrhagic fever (CCHF) is a severe disease of humans caused by CCHF virus  
28 (CCHFV), a biosafety level (BSL)-4 pathogen. Ticks of the genus *Hyalomma* are the viral reservoir  
29 and they represent the main vector transmitting the virus to its hosts during blood feeding. We have  
30 previously shown that CCHFV can persistently infect *Hyalomma*-derived tick cell lines. However,  
31 the mechanism allowing the establishment of persistent viral infections in ticks is still unknown.  
32 Hazara virus (HAZV) can be used as a BSL-2 model virus instead of CCHFV to study virus/vector  
33 interactions. To investigate the mechanism behind the establishment of a persistent infection, we  
34 developed an *in vitro* model with *Hyalomma*-derived tick cell lines and HAZV. As expected,  
35 HAZV, like CCHFV, persistently infects tick cells without any sign of cytopathic effect, and the  
36 infected cells can be cultured for more than three years. Most interestingly, we demonstrated the  
37 presence of short viral-derived DNA forms (vDNAs) after HAZV infection. Furthermore, we  
38 demonstrated that the antiretroviral drug AZT could inhibit the production of vDNAs, suggesting  
39 that vDNAs are produced by an endogenous retrotranscriptase activity in tick cells. Moreover, we  
40 collected evidence that vDNAs are continuously synthesized, thereby downregulating viral  
41 replication to promote cell survival. Finally, vDNAs were also detected in CCHFV-infected tick  
42 cells. In conclusion, vDNA synthesis might represent a strategy to control the replication of RNA  
43 viruses in ticks allowing their persistent infection.

44

45

46 **IMPORTANCE.**

47 Crimean-Congo hemorrhagic fever (CCHF) is an emerging tick-borne viral disease caused by  
48 CCHF virus (CCHFV). Ticks of the genus *Hyalomma* can be persistently infected with CCHFV  
49 representing the viral reservoir, and the main vector for viral transmission. Here we showed that  
50 tick cells infected with Hazara virus, a nonpathogenic model virus closely related to CCHFV,  
51 contained short viral-derived DNA forms (vDNAs) produced by endogenous retrotranscriptase

52 activity. vDNAs are transitory molecules requiring viral RNA replication for their continuous  
53 synthesis. Interestingly, vDNA synthesis seemed to be correlated with downregulation of viral  
54 replication and promotion of tick cell viability. We also detected vDNAs in CCHFV-infected tick  
55 cells suggesting that they could represent a key element in the cell response to nairovirus infection  
56 and might represent a more general mechanism of innate immunity against RNA viral infection.

57 **Keywords:**

58 Crimean–Congo hemorrhagic fever virus, Hazara virus, tick cell line, tick, viral-derived DNA  
59 forms, Orthonairovirus, tick-borne disease

60

61 **INTRODUCTION**

62 Crimean-Congo hemorrhagic fever (CCHF) is an emerging tick-borne viral disease widely  
63 distributed across Africa, Southern Europe, the Middle East and Asia (1). It is considered to be one  
64 of the major emerging disease threats spreading to, and also within, the European region following  
65 increasing circulation of its main vectors, ticks of the genus *Hyalomma* (2). Furthermore, CCHF is  
66 included in the WHO List of Blueprint priority diseases (3). CCHF is caused by Crimean-Congo  
67 hemorrhagic fever virus (CCHFV), which belongs to the genus *Orthonairovirus* of the recently-  
68 established family *Nairoviridae* (4). CCHFV is characterized by an enzootic cycle in asymptomatic  
69 mammals and ticks, while human infection represents an accidental event. Although 85% of human  
70 cases are subclinical, in symptomatic patients infection begins with fever and other nonspecific  
71 clinical signs, and can progress to a serious hemorrhagic syndrome with a case fatality rate up to  
72 30% (5, 6).

73 Although CCHFV has been detected in many tick species, *Hyalomma* ticks represent the main  
74 vectors of the virus and the natural reservoir. In fact, *Hyalomma* ticks feeding on a viremic host  
75 become persistently infected with CCHFV, the virus survives through the subsequent stages of the  
76 tick life cycle, and transovarial transmission occurs in this genus (7). To date, very limited  
77 information is available about the replication and persistence of CCHFV in ticks due to the

78 requirement for the virus to be handled in high-containment laboratories, compounded by the  
79 difficulty in manipulation of infected ticks in a biosafety level (BSL)-4 facility (7, 8). However, we  
80 have recently developed a CCHFV infection model based on embryo-derived *Hyalomma*  
81 *anatolicum* cell lines, providing the opportunity to study virus-vector interaction in an easier-to-  
82 handle *in vitro* system (9, 10).

83 Hazara virus (HAZV), originally isolated from a pool of adult *Ixodes redikorzevi* ticks removed  
84 from a vole in Pakistan (11), is a member of the family *Nairoviridae* and is closely related to  
85 CCHFV. Although genome sequence analyses clustered CCHFV and HAZV in different species,  
86 HAZV was classified in the same serogroup as CCHFV, based on antibody cross-reactivity between  
87 antigens of the two viruses (12, 13). Studies reported that CCHFV and HAZV have similar  
88 biological characteristics in terms of replication, interaction with cellular partners, and modulation  
89 of apoptosis (14–21). Although HAZV is able to simulate a disease similar to that induced by  
90 CCHFV in an interferon-deficient mouse model, it has never been associated with human disease  
91 and is considered a non-pathogenic virus that can be manipulated under BSL-2 conditions (22).

92 In the present study, we investigated virus/host interactions and possible mechanisms allowing the  
93 establishment of a persistent infection in ticks by applying HAZV, as a safe surrogate for CCHFV,  
94 to our tick cell line model. Interestingly, we showed that viral infection is associated with the  
95 synthesis of small viral-derived DNA forms (vDNAs), produced by a cellular reverse-transcriptase  
96 activity, that are required to suppress viral replication and thereby maintain tick cell viability.

97 Finally, we confirmed that vDNAs were also detectable in CCHFV-infected tick cells supporting  
98 the hypothesis that they could represent a key element in the cellular response to nairovirus  
99 infection. vDNAs might be involved in a general mechanism of innate immunity to counteract RNA  
100 virus infections in ticks.

101

102

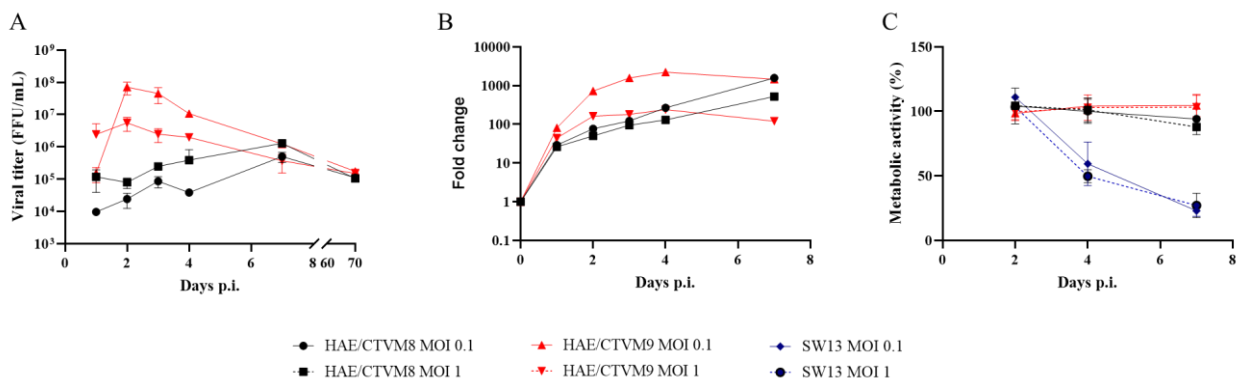
103

104 **RESULTS**

105 **HAZV persistently infects *Hyalomma*-derived tick cell lines.** To investigate whether  
106 HAZV is able to productively infect *Hyalomma*-derived tick cell lines, the *H. anatolicum* cell lines  
107 HAE/CTVM8 and HAE/CTVM9 (23) were infected with HAZV at a multiplicity of infection  
108 (MOI) of 0.1 or 1.0. Viral replication was monitored by progeny titration and by evaluating the  
109 intracellular viral RNA yield using a quantitative real-time RT-PCR (qRT-PCR) approach. Titration  
110 of viral progeny in supernatants collected on days 1, 2, 3, 4 and 7 post infection (p.i.) showed that  
111 HAZV can productively infect *H. anatolicum* cells (Fig. 1A). The kinetics of viral progeny release  
112 were slightly different in the two cell lines; production of infectious viral particles was faster in  
113 HAE/CTVM9 than in HAE/CTVM8 cells. However, at 7 days p.i., prior to subculturing the  
114 infected cells, similar HAZV titers were observed in both cell lines (Fig. 1A). No viral particles  
115 were detected in supernatants of mock-infected cells (data not shown). The qRT-PCR results  
116 confirmed that replication of HAZV was slower in HAE/CTVM8 than in HAE/CTVM9 cells (Fig.  
117 1B). Starting from day 7 p.i., infected tick cell cultures were split every 7-10 days. HAZV was  
118 detected in subcultures by viral titration for 70 days suggesting the establishment of a persistent  
119 infection (Fig 1A).

120 To rule out the possibility that the different pattern of viral replication observed at the early  
121 time points (days 2-4 p.i.) was independent of an effect of the virus on cell viability, HAZV-  
122 infected HAE/CTVM8 and HAE/CTVM9 cells were monitored by phase-contrast microscopy and  
123 an MTT assay was used to evaluate cellular metabolic activity as a measure of viability. HAZV-  
124 infected human SW13 cells were used as positive control cells killed by the virus. In fact, HAZV  
125 efficiently replicates in SW13 cells (14, 17) producing a robust cytopathic effect as described for  
126 CCHFV (18). As expected, the metabolic activity of SW13 cells rapidly decreased over time after  
127 viral infection for both MOIs tested (Fig. 1C). In contrast, microscopic analysis of tick cell cultures  
128 (data not shown) and MTT assay performed at 2, 4, and 7 days p.i. did not detect any significant

129 effect on the tick cells even at day 7 (Fig. 1C) suggesting that the HAZV infection did not affect  
 130 tick cell viability.

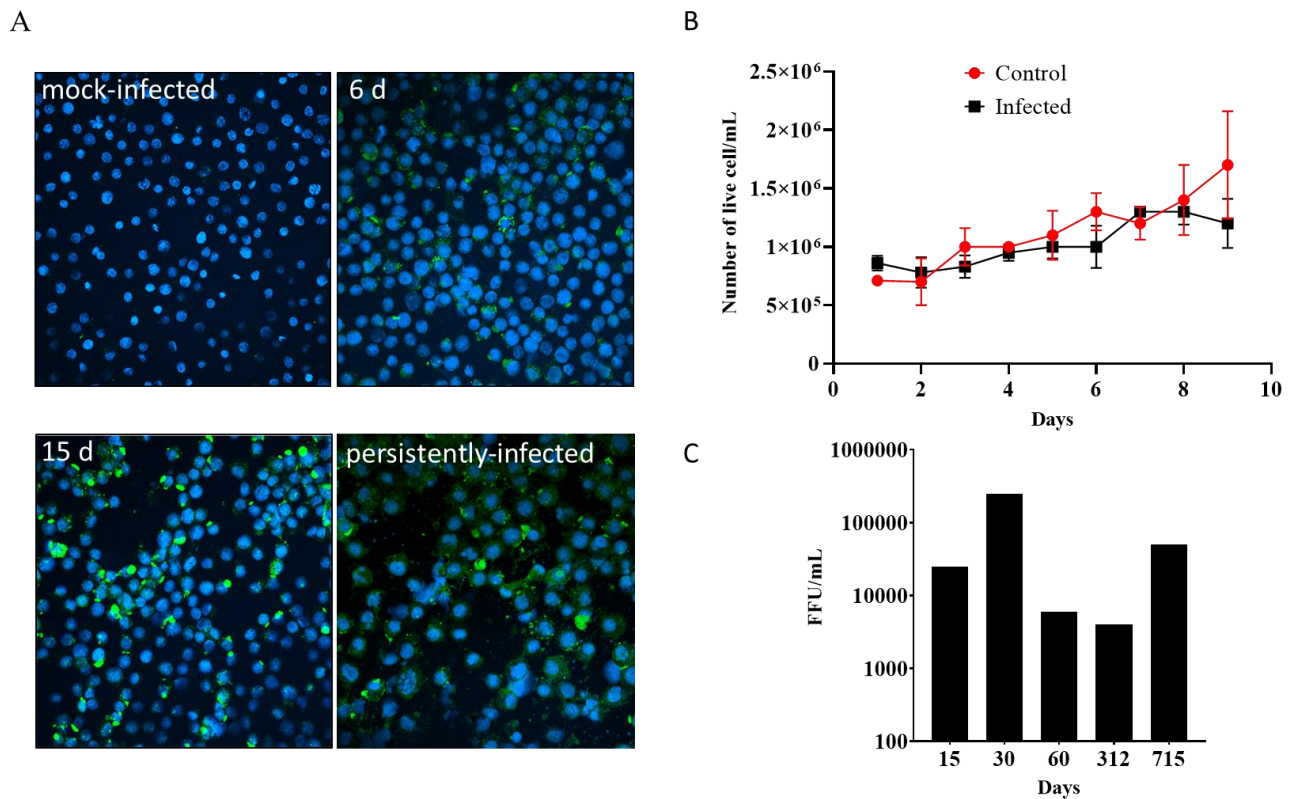


131  
 132 **Figure 1. Hazara virus (HAZV) productively infects *Hyalomma anatolicum* tick cells without**  
 133 **cytopathic effects.** (A and B) HAE/CVTVM8 and HAE/CTVM9 cells were infected at MOI 0.1 or  
 134 MOI 1.0. At the indicated time points: (A) infectious viral particles in the supernatant were titrated  
 135 in Vero cells, error bars = S.D.; (B) the relative increase of viral RNA in the infected cells was  
 136 evaluated by qRT-PCR. Data are the results of a representative experiment. (C) Tick cell lines and  
 137 human SW13 cells were infected with HAZV at MOI 0.1 and 1.0 and cell metabolism was  
 138 evaluated using the MTT assay at the indicated time points. Data (mean  $\pm$  SD, N = 3 independent  
 139 experiments) are percentages of optical density of infected cells with respect to that of uninfected  
 140 cells set as 100%.

141  
 142 Taking into account that HAE/CTVM8 cells showed similar kinetics of replication for HAZV and  
 143 CCHFV (9) and grew more reliably in our hands than HAE/CTVM9 cells, we focused our attention  
 144 on this cell line for the subsequent experimental steps.

145 To further characterize the generation of the persistently-infected HAE/CTVM8 cells, we firstly  
 146 evaluated the percentage of HAZV-infected cells during the initial stages of infection by  
 147 challenging HAE/CTVM8 cells with HAZV at MOI 0.1. Next, we evaluated infected cells over  
 148 time by immunostaining of viral nucleoprotein (N). As shown in Figure 2A, the proportion of N-  
 149 expressing cells increased from ~43% at day 6 p.i. to ~62% at day 15 p.i., while at later time points,

150 when cells are persistently infected, almost all cells stained positive (Fig 2A – panel showing  
 151 persistently infected cells). In addition, we confirmed that HAZV did not kill infected cells, as  
 152 demonstrated by similar growth kinetics of virus-infected and mock-infected control cells (Fig. 2B).  
 153 These observations suggest that the virus was slowly spreading throughout the culture from an  
 154 initially low number of infected cells. The persistence of HAZV was further confirmed in infected  
 155 HAE/CTVM8 cells by RT-PCR at 15, 30, 60, 312, and 715 days p.i. (data not shown) and by the  
 156 titration of infectious viral progeny (Fig. 2C) indicating continued active viral replication. Persistent  
 157 infection of HAE/CTVM8 cells was achieved on three independent occasions and one of the  
 158 persistently-infected cultures was maintained for more than three years.



159  
 160 **Figure 2. Hazara virus (HAZV) infects *Hyalomma anatolicum* tick cells and does not affect cell**  
 161 **viability.** HAE/CTVM8 cells were infected with HAZV at MOI 0.1 and (A) infected and mock-  
 162 infected cells were monitored by N protein immunostaining at 6 (6d) and 15 (15d) days post  
 163 infection (p.i.) and at > 1 year of culture (persistently infected) while (B) the number of live cells in  
 164 infected and mock-infected control cultures were determined every day up to day 9 p.i. by trypan

165 blue exclusion (three independent experiments) and (C) long term viral progeny release by HAZV-  
166 infected HAE/CTVM8 cells was determined by titration in Vero cells. (A) and (C) are  
167 representative of the establishment of one persistently-infected cell lines.

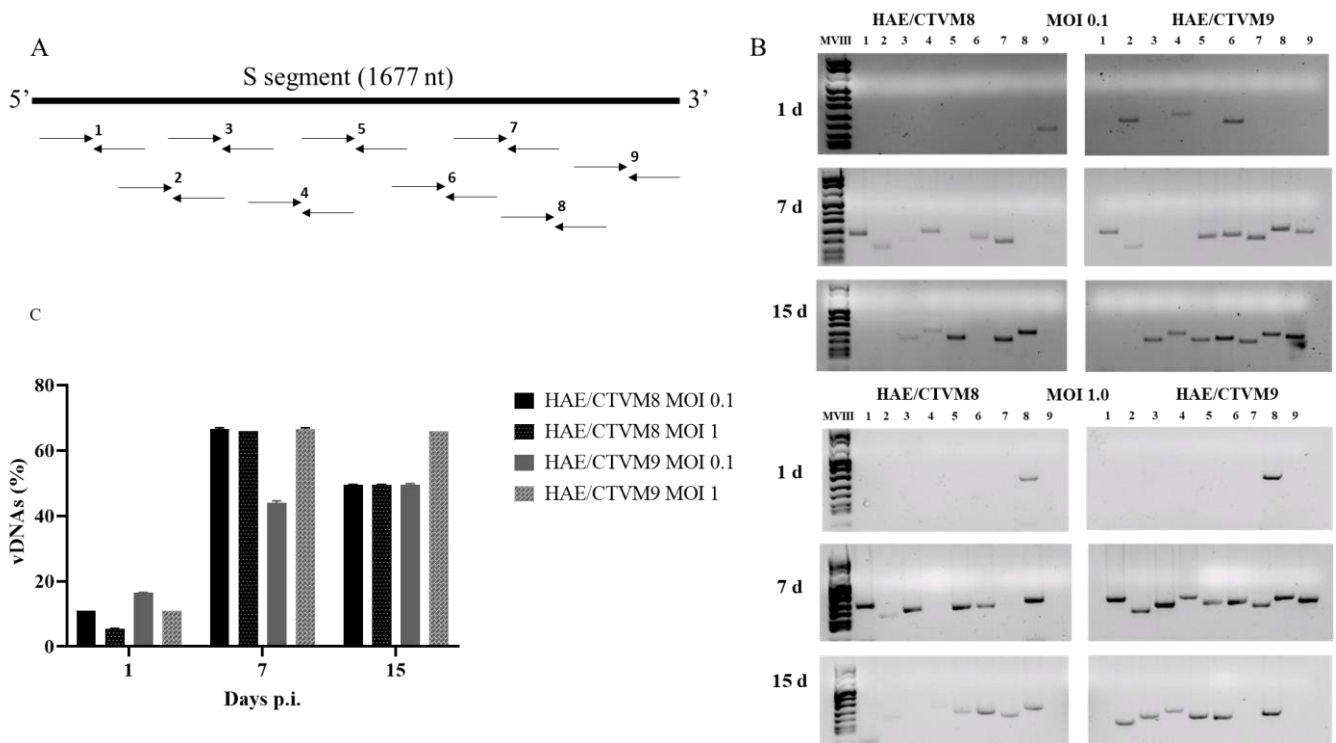
168

169 **Viral-derived DNA forms are detectable in *de novo* infected and persistently-infected tick**  
170 **cells.** It has been recently reported that in some insect cells RNA virus infection is associated with  
171 the synthesis of vDNAs that are involved in the establishment of persistent infection (24, 25). To  
172 determine whether HAZV infection of tick cells was associated with the formation of vDNAs,  
173 HAE/CTVM8 and HAE/CTVM9 cell were infected with HAZV at MOI 0.1 and 1.0 and the  
174 formation of vDNAs was evaluated by PCR. To this end, nine pairs of primers, designed to amplify  
175 overlapping sequences of 152-237 bp covering the S segment of the HAZV genome, were adopted  
176 (Fig. 3A). Specific PCR amplicons were already obtained from total DNA extracted from infected  
177 tick cells at day 1 p.i., with a maximum number of fragments detected at 7 days p.i. (Fig. 3B-C). No  
178 vDNAs were detected in mock-infected tick cells or, more significantly, in HAZV-infected  
179 mammalian Vero cells (data not shown). Furthermore, while RNase treatment of infected cell DNA  
180 extracts did not affect amplification of vDNAs, when DNase was added no PCR products were  
181 detected (data not shown). Finally, when combining the primers of contiguous amplicons, we did  
182 not detect fragments larger than ~240 bp, suggesting that each vDNA represent only a small portion  
183 of the viral genome segment, and that neither long fragments nor the entire genome segment were  
184 synthesized (data not shown). Overall, these results suggest that vDNAs are small DNA fragments  
185 likely derived from the HAZV genome.

186 Interestingly, vDNAs were constantly detectable in persistently-infected tick cell cultures, as the  
187 presence of vDNAs was periodically confirmed by PCR (up to 10 times per year; data not shown)  
188 suggesting that they either represent stable molecules or are continuously synthesized during cell  
189 culture.

190





192

193 **Figure 3. Detection of vDNAs in *Hyalomma anatolicum* tick cells infected with Hazara virus**194 **(HAZV) at MOI 0.1 and 1. (A)** Schematic representation of nine pairs of primers designed on the

195 genomic S segment of HAZV, used for the detection of vDNAs; (B) Example of vDNAs detected

196 using the nine primer pairs at 1 (upper panel), 7 (middle panel) and 15 (lower panel) days p.i. in

197 HAZV-infected HAE/CTVM8 and HAE/CTVM9 cells; (C) Frequency of vDNA production in the

198 same tick cells. Data (mean  $\pm$  SD, N = 3 independent experiments) are percentages of vDNAs with

199 respect to the maximum number of detectable amplicons (n=9), set as 100%, for each sample.

200

201 **vDNA synthesis depends on viral RNA replication and is mediated by a cellular reverse-**202 **transcriptase activity**

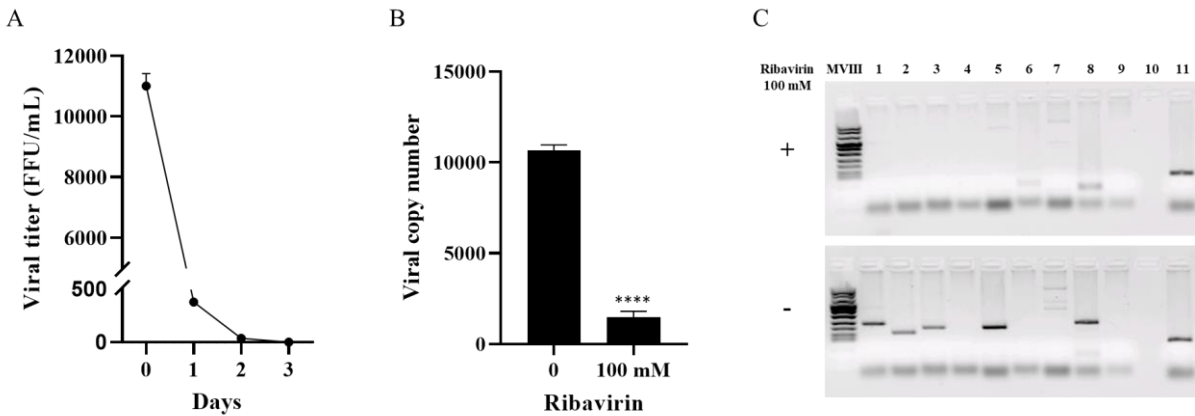
203 To investigate whether viral RNA replication is required for vDNA synthesis, HAE/CTVM8

204 cells were infected with UV-inactivated HAZV. Three days later, total DNA was extracted and

205 submitted to PCR analyses and no vDNAs were detected (data not shown). Furthermore,

206 HAE/CTVM8 cells, persistently infected for at least 6 months, were treated with ribavirin (100

207 mM), a drug known to inhibit viral genome replication. As expected and shown in Figure 4 A and B,  
 208 viral progeny production was suppressed and the yield of intracellular viral RNA decreased. In this  
 209 experimental condition, at 72 h post treatment, vDNAs disappeared suggesting that viral RNA  
 210 replication is required for vDNA synthesis (Fig 4C).



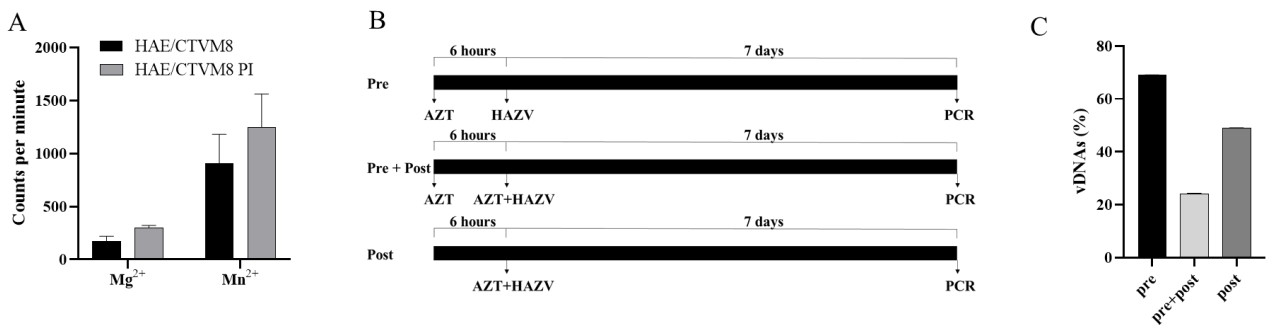
211

212 **Figure 4. Effect of ribavirin treatment on Hazara virus (HAZV) replication in persistently-**  
 213 **infected *Hyalomma anatolicum* tick cells.** HAE/CTVM8 cells were treated with 100 mM ribavirin  
 214 and viral replication was evaluated: (A) at different time points by viral titration; (B) at 72 h post  
 215 treatment by qRT-PCR. Data are mean  $\pm$  SD of three independent experiments. \*\*\*\* p<0.0001. (C)  
 216 Furthermore, production of vDNAs was suppressed by the ribavirin treatment (Lines 1-9: PCR  
 217 specific for vDNAs, line 10: negative control, line 11: positive tick DNA extraction control).

218

219 In the case of RNA viruses lacking a viral enzyme able to convert genomic RNA to DNA,  
 220 the formation of vDNAs could be due to the presence of endogenous reverse transcriptases (RTs)  
 221 encoded by retrotransposons and/or endogenous retroviruses integrated into the genome of tick cells.  
 222 By performing an RT assay, we detected a clear  $Mn^{2+}$  dependent RT-activity in HAE/CTVM8 cell  
 223 lysates, with a slightly higher level in HAE/CTVM8 cells persistently infected with HAZV (cells  
 224 cultured for more than 6 months) compared to uninfected cells (Fig. 5A). Furthermore, to  
 225 demonstrate that vDNAs were synthesized by cellular RT activity, we treated HAE/CTVM8 cells  
 226 with the nucleoside RT inhibitor azidothymine triphosphate (AZT). Specifically, 5 mM AZT was

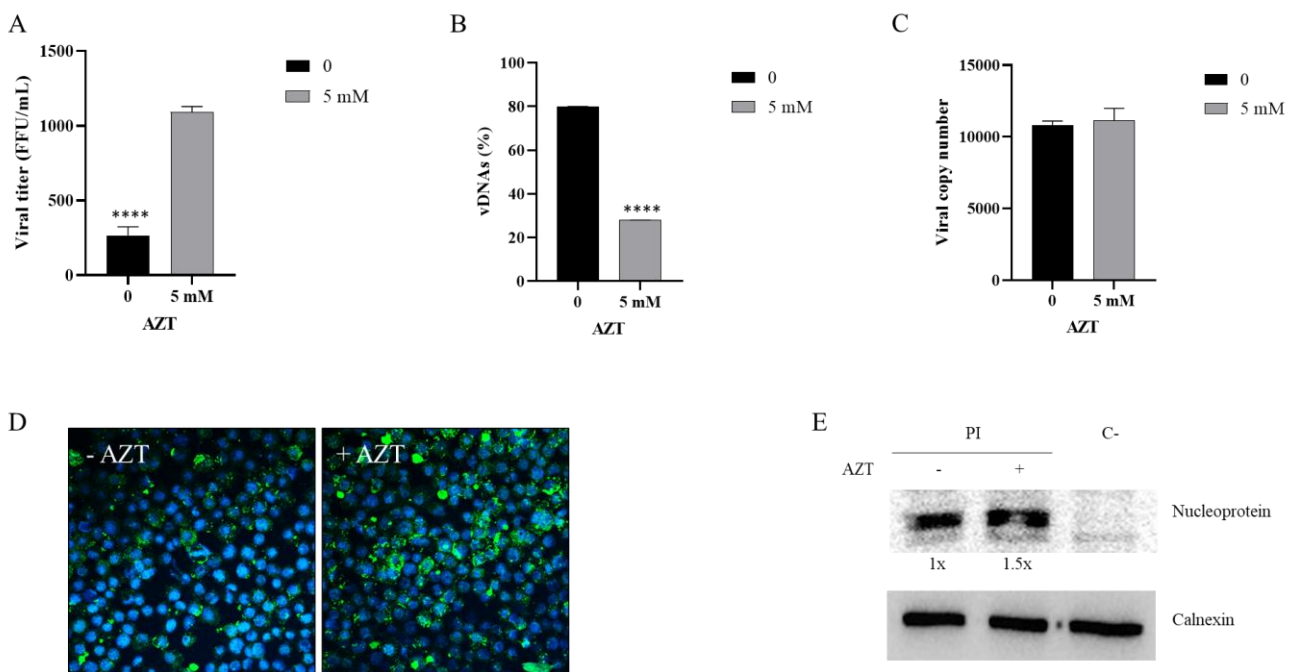
227 selected, as this concentration did not significantly affect cell viability (see next paragraph) and had  
 228 been already adopted to treat insect cells (24, 25). In addition, three different schedules of AZT  
 229 administration were adopted: 1) 6 h before virus infection; 2) at the time of viral infection; 3) 6 h  
 230 before virus infection as well as at the time of infection (Fig. 5B). As shown in Fig. 5C, while a  
 231 reduction up to 30% in vDNA yield was observed when cells were treated with AZT before viral  
 232 infection (experimental condition 1), this reduction increased up to 50% when the drug was added  
 233 during the viral adhesion step (experimental condition 2). A stronger effect (roughly 70% reduction)  
 234 resulted from the combination of the two treatments (experimental condition 3). Overall, these  
 235 results suggest that a cellular RT activity is required for the synthesis of vDNA.



236  
 237 **Figure 5. A cellular reverse transcriptase (RT) activity is involved in vDNA synthesis in**  
 238 ***Hyalomma anatolicum* tick cells infected with Hazara virus (HAZV).** (A) Detection of RT  
 239 activity in uninfected HAE/CTVM8 cells and HAE/CTVM8 cells persistently infected with HAZV  
 240 (HAE/CTVM8+) using Mg<sup>2+</sup> or Mn<sup>2+</sup> as enzyme cofactor. Data are mean ± SD of three  
 241 independent experiments. (B) Schedule of azidothymine triphosphate (AZT) treatment of  
 242 HAE/CTVM8 cells before (pre) or simultaneously with (post) HAZV infection. (C) Effect of AZT  
 243 treatment of HAZV-infected HAE/CTVM8 cells on vDNA synthesis at 7 days p.i. Data (mean ± SD,  
 244 N = 3 independent experiments) are percentages of vDNAs detected in AZT-treated cells with  
 245 respect to the vDNAs detected in the untreated cells, set as 100%.

246  
 247 **vDNAs promote suppression of viral particle production and survival of HAZV-infected tick**  
 248 **cells**

249 To evaluate the effect of vDNAs on HAZV infection in tick cells, we treated persistently-  
 250 infected (>1 year of culture) HAE/CTVM8 cells with 5 mM AZT. Seventy-two hours later, the viral  
 251 titer obtained from treated cells was roughly 4 times higher than the one obtained from untreated  
 252 cells. Furthermore, the number of vDNAs in treated cells was roughly one-third of that seen in the  
 253 untreated cells (Fig. 6A-B). By contrast, the yield of intracellular viral RNA was not affected by  
 254 AZT treatment, suggesting that AZT does not interfere with viral genome replication (Fig. 6C).  
 255 However, immunostaining (Fig. 6D) revealed a clear increase of the amount of HAZV N protein  
 256 (increase of fluorescence intensity) in AZT-treated cells, which was quantified by western blotting  
 257 as 1.5 times greater than that in control cells (Fig. 6E), suggesting a higher level of N protein  
 258 synthesis.

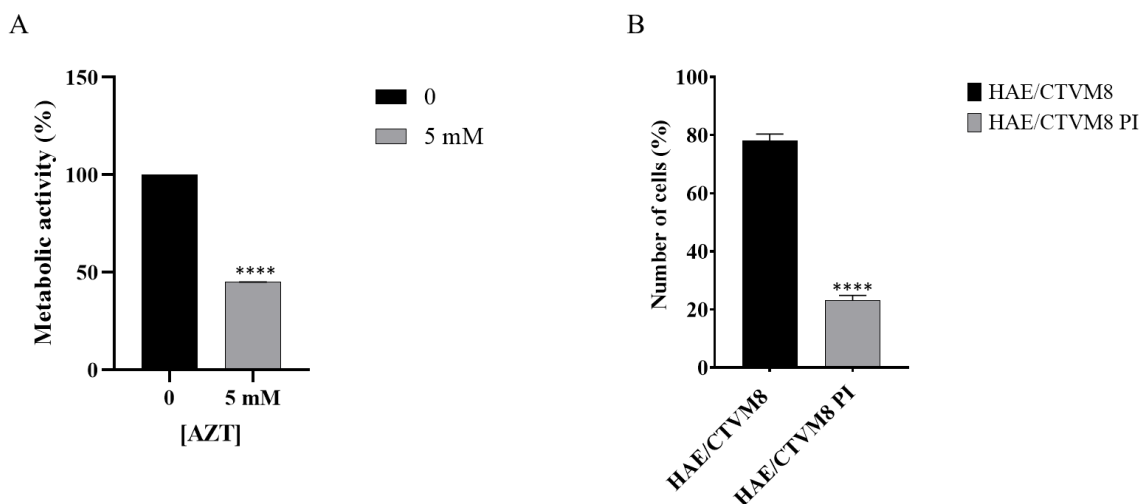


259  
 260 **Figure 6. Azidothymine triphosphate (AZT) treatment of *Hyalomma anatolicum***  
 261 **HAE/CTVM8 cells persistently infected with Hazara virus (HAZV) induces an increase in**  
 262 **viral replication and decrease in cell metabolism.** Cells were treated with 5 mM AZT and  
 263 incubated for 72 h. Then (A) the viral progeny was quantified by virus titration; (B) the presence of  
 264 vDNAs was evaluated by PCR and, (C) the yield of the intracellular viral RNA was quantified by  
 265 qRT-PCR. Data are mean  $\pm$  SD of three independent experiments. \*\*\*\* p<0.0001. The

266 nucleoprotein of HAZV was (D) detected by immunostaining and (E) quantified by western blot to  
267 be 1.5 x grater in persistently-infected HAE/CTVM8 cells treated with 5 mM AZT compared to  
268 untreated cells. PI = persistently-infected cells; C- = uninfected control cells.

269

270 Interestingly, an MTT assay showed a significant decrease in the metabolism of AZT-treated cells  
271 (Fig. 7A), associated with the increase in viral titer. To demonstrate that the reduction in cell  
272 metabolism was associated with viral-mediated cell death, uninfected and persistently-infected  
273 HAE/CTVM8 cells were treated with AZT and the number of live cells was counted by trypan blue  
274 exclusion assay. Although the AZT caused a slight reduction in the number of uninfected cells over  
275 a 72 h period, a significant decrease in live cell numbers was observed only in persistently-infected  
276 cells (Fig. 7B).



277

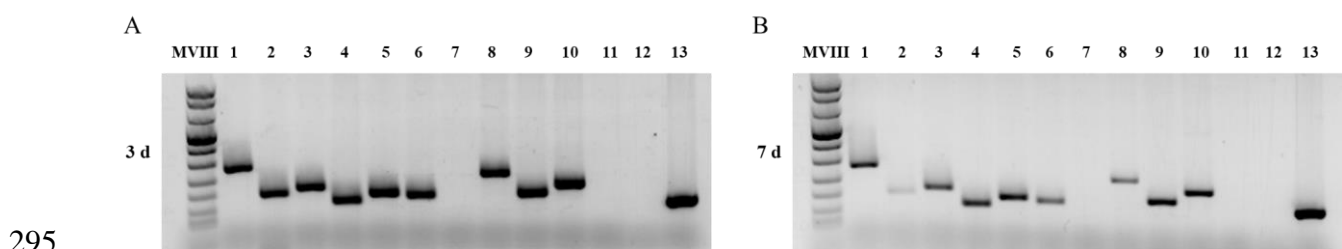
278 **Figure 7. Treatment of *Hyalomma anatolicum* HAE/CTVM8 cells with azidothymine**  
279 **triphosphate (AZT) induces death in persistently-infected cells.** (A) Tick cells persistently  
280 infected with Hazara virus were mock-treated or treated with 5 mM AZT, then cell metabolism was  
281 measured using the MTT assay at 72 h post infection (p.i.). (B) Uninfected (HAE/CTVM8) and  
282 persistently-infected (HAE/CTVM8 PI) tick cells were treated with 5 mM AZT, then cell viability  
283 was determined by trypan blue dye exclusion test at 72 h p.i.. Data are mean  $\pm$  SD of three  
284 independent experiments. \*\*\*\* p<0.0001.

285 In conclusion, our data suggest that vDNAs might contribute to controlling HAZV infection in tick  
286 cells by suppressing the production of infectious viral progeny and, thereby, promoting the survival  
287 of infected cells.

288

### 289 vDNAs are detectable in CCHFV-infected HAE/CTVM8 tick cells

290 We have previously demonstrated that CCHFV can persistently infect *Hyalomma*-derived  
291 tick cell lines (9). To demonstrate that CCHFV infection induces vDNA formation in tick cells,  
292 HAE/CTVM8 cells were infected with CCHFV at MOI 0.1 and harvested at 3 and 7 days p.i.. As  
293 for HAZV, we designed a panel of primers covering the entire S segment of CCHFV and the PCR  
294 analyses on total DNA extracted from infected cells demonstrated the presence of vDNAs (Fig. 8).



295  
296 **Figure 8. Detection of vDNAs in *Hyalomma anatolicum* HAE/CTVM8 cells infected with**  
297 **Crimean-Congo hemorrhagic fever virus (CCHFV).** HAE/CTVM8 cells were infected with  
298 CCHFV at MOI 0.1. Three (left panel) and seven (right panel) days after infection, total DNA was  
299 extracted and vDNAs were detected by PCR. Lines 1-11: PCR specific for vDNAs, line 12:  
300 negative control, line 13: positive tick DNA extraction control.

301

302 This result suggests that vDNA production could be a common tick cellular response following  
303 RNA virus infection, as reported for some insects (26).

304

### 305 DISCUSSION

306 CCHFV is the most important and globally-widespread tick-borne hemorrhagic fever virus and its  
307 emergence and re-emergence highlight the importance of this infectious agent for human health (1).

308 Despite the rapid increase in knowledge of viral biology and the development of diagnostic tools in  
309 the last decade (2), there is still a large gap in the characterization of virus/vector interaction.  
310 We and others have shown that CCHFV can persistently infect ticks and tick cell lines without  
311 deleterious effects (7, 9, 10, 27, 28); however, the mechanism allowing the persistent infection of  
312 CCHFV (and other tick-borne viruses) in ticks has not yet been characterized.

313 In the present study, we adopted HAZV as a non-pathogenic surrogate for CCHFV, with the aim of  
314 studying the mechanisms involved in the establishment of persistent infection of tick vectors.

315 Firstly, we showed that HAZV replicates productively in cell lines derived from tick of a genus  
316 (*Hyalomma*) that was never reported to function as a vector for HAZV (29). In addition, the HAZV  
317 infection did not appear to be cytopathic for tick cells and persisted for a long time, as previously  
318 reported in the case of CCHFV and other tick-borne viruses (9, 10, 27, 30–32). It is notable that  
319 HAZV showed kinetics of replication in *H. anatolicum* cell lines faster than those previously  
320 reported for CCHFV in the same cell lines (9, 27) and produced higher viral titers, suggesting that  
321 *Hyalomma* ticks could support HAZV infection (27).

322 Previously, Goic and co-workers demonstrated that short vDNAs were detected *in vitro* and *in vivo*  
323 in insect cells infected by RNA viruses and that they were involved in the control of virus  
324 replication allowing persistent infection of cultured cells and insects (24, 25). Remarkably, we  
325 detected vDNAs in HAZV-infected tick cells from as early as 24 h p.i.. Considering that  
326 nairoviruses do not encode a viral RT, the RT-activity required for vDNA synthesis could be  
327 provided by endogenous cellular sequences (i.e. retrotransposons and retroviral sequences). No  
328 genome sequences are as yet available for any *Hyalomma* spp. ticks; however a reverse  
329 transcriptase-like protein has been described in *Amblyomma americanum* (UniProtKBQ49P04)  
330 while RT activity was detected in three *Ixodes scapularis* embryo-derived cell lines (33), thus  
331 supporting the possibility of RT expression also in *Hyalomma* derived cell lines. In fact, we  
332 detected Mn<sup>2+</sup> dependent RT-activity in HAE/CTVM8 cell lysates, and experiments with the RT

333 inhibitor AZT showed that RT is involved in vDNA synthesis in tick cells, as described for insect  
334 cells (24, 25).

335 Moreover, our data showed that vDNAs are always detectable in persistently-infected tick cells and  
336 the S segment can be fully used as template for their synthesis. In contrast, Nag and co-workers  
337 reported that only two regions of the S segment of La Crosse virus (LACV), another member of the  
338 order *Bunyavirales*, were detectable in infected C6/36 insect cells (34). This apparent discrepancy  
339 between HAZV and LACV might be due to biological differences between the two viruses. On the  
340 other hand, it should be taken into account that those authors adopted a different PCR strategy, not  
341 based on multiple small overlapping amplicons. Furthermore, they analyzed vDNA presence only at  
342 one time point after viral infection, a choice that might have negatively impacted the efficiency of  
343 detection (34). Interestingly, we observed that vDNA amplification depends on active viral RNA  
344 replication, suggesting that vDNAs are not stable but are continuously synthesized during the  
345 persistent infection of tick cells.

346 Reports on insect RNA viruses suggest that vDNAs may be produced via template-switching events,  
347 when the RT switches from the retro-elements template to viral RNA forming linear and episomal  
348 vDNA-retrotransposon chimeric molecules, while integration events into the genome are rare (24,  
349 25, 35, 36). However, the integration of viral sequences into the arthropod genome, although  
350 infrequently detected to date, is considered important in virus/vector co-evolution (10, 37–39). In  
351 fact, many bunya- and othomyxo-like sequences have been identified in the *I. scapularis* genome  
352 suggesting that these viruses can produce vDNAs in ticks and occasionally integrate into the  
353 genome of germline cells (40).

354 The modulation of virus replication mediated by vDNAs in insects is based on an RNAi  
355 mechanism; it has been shown that vDNAs are transcribed and used as templates for the synthesis  
356 of short RNAs that suppress viral replication (24, 25, 34, 36, 41). Our data are compatible with this  
357 mechanism. In fact, we observed that: i) the proportion of infected cells increased over time during  
358 the infection while viral titer decreased; ii) the inhibition of vDNA synthesis by AZT treatment was



359 associated with an increase in nucleoprotein yield and viral titer without any effect at the level of  
360 intracellular viral RNA, thus suggesting post-transcriptional regulation. However, at this stage, a  
361 contribution of specific effects on viral genome replication/transcription efficiency cannot be fully  
362 ruled out.

363 The above-described model of vDNA production is compatible with the requirement of active viral  
364 RNA replication for vDNA synthesis; continuous virus replication allows the production of RNA  
365 templates and the chance of switching events producing new vDNAs. On the other hand, vDNAs  
366 may mediate a suppressive effect on virus replication, reducing virus proteins and progeny release,  
367 thus inducing an equilibrium between virus replication and generation of new vDNAs.

368 More interestingly, inhibition of vDNA synthesis induced a reduction in cell viability, as showed by  
369 MTT and by the proportion of live cells. According to the literature on insect RNA viruses, increase  
370 of viral assembly and budding could be associated with a cytotoxic effect, negatively affecting cell  
371 survival (24, 25).

372 Although more research is required to further characterize the biology of vDNA production and  
373 function, our *in vitro* data supported the view that vDNAs are linked to the establishment of  
374 persistent viral infections, reducing the production of viral progeny and protecting tick cells from  
375 deleterious effects. *In vivo* experiments could investigate the relevance of vDNA inhibition for tick  
376 survival, as demonstrated in the case of mosquitoes infected with arboviruses (24, 25). Indeed, the  
377 development of tools to interfere with vDNA synthesis might represent a strategy to reduce the  
378 fitness of infected ticks and lower the risk of transmission of the virus in endemic areas.

379 In conclusion, we show for the first time that vDNAs are detectable in tick cells infected with  
380 HAZV and CCHFV. As described for insect-borne RNA viruses, vDNAs seem to be associated  
381 with the establishment of persistent infection in ticks, which are classified in a different subphylum  
382 of the *Arthropoda* from insects. Also, in this context vDNAs appear to control viral replication and  
383 promote cell survival, thus allowing persistence of the virus in the environment. Overall these

384 findings suggest that vDNA synthesis might represent a common strategy to control viral infections  
385 in arthropods.

386

## 387 **MATERIALS AND METHODS**

388 **Cells and viruses.** All culture media and supplements were obtained from Gibco unless otherwise  
389 indicated. SW13 cells (human adrenal cortex adeno-carcinoma cells, ATCC® CCL-105™), were  
390 cultured in Leibovitz's L-15 medium (L-15) supplemented with 10% heat-inactivated fetal bovine  
391 serum (FBSi) and 100 U/mL penicillin and 100 µg/mL streptomycin (p/s). Vero cells (African  
392 green monkey kidney cells, ATCC® CCL-81) were grown in Dulbecco's modified Eagle's medium  
393 (D-MEM) containing 10% FBSi and p/s. Vero cells were maintained at 37 °C in a humidified  
394 atmosphere of 5 % CO<sub>2</sub> in air while SW13 cells were maintained at 37 °C in ambient air.

395 The *H. anaticum* embryo-derived cell lines HAE/CTVM8 and HAE/CTVM9 were grown in,  
396 respectively, L15/H-Lac medium (equal volumes of L-15 supplemented with 10% tryptose  
397 phosphate broth [TPB] and Hank's balanced salt solution with 0.5% lactalbumin hydrolysate  
398 [Sigma]) and L-15/MEM medium (equal volumes of L-15 and Minimal Essential Medium with  
399 Hank's salts supplemented with 10% TPB), both supplemented with 2 mM L-glutamine, 20% FBSi  
400 and p/s, and incubated in sealed flat-sided culture tubes (Nunc, Thermo-Fisher Scientific) in  
401 ambient air at 32 °C (23).

402 Uninfected and HAZV-infected SW13 and tick cell metabolic activity was tested with an assay  
403 based on the reduction of a tetrazolium salt (MTT Cell Proliferation Assay ATCC ® 30-1010K™)  
404 in a 96-well plate format according to the manufacturer's instructions. Tick cells were grown in  
405 sealed 96-well plates for the MTT assay.

406 The HAZV JC280 and the CCHFV IbAr10200 strains produced in SW13 cells were used in the  
407 experiments (21).

408

409 **Viral stock preparation.** SW13 cells were seeded in T75 flasks and then infected with HAZV or  
410 CCHFV (MOI of ~ 0.1). At 48-72 h p.i., supernatants were collected, centrifuged at  $896 \times g$  for 10  
411 min, then 10-fold serially diluted in L-15 with 2% FBSi and titrated on Vero cells in 96-well plates.  
412 After 24 h incubation, cells were fixed with methanol-acetone and stained for immunofluorescence  
413 assay using a rabbit polyclonal anti-CCHFV nucleoprotein antibody (21), that also recognized  
414 HAZV-N, and Alexa Fluor<sup>TM</sup> 488 goat anti-rabbit IgG (Invitrogen), according to the  
415 manufacturer's instructions. The fluorescent foci in each well were counted and viral titer was  
416 expressed as focus-forming units per mL (FFU)/mL.

417

418 **Infection of tick cell lines.** Tick cells ( $2 \times 10^6$ ) were seeded in flat-sided tubes and cultured for 48 h  
419 in 2.5 mL of complete medium. Then, 1.5 mL medium was removed and retained, and cells were  
420 incubated for 1 h with HAZV, at the appropriate MOI, in a final volume of ~1 mL of complete  
421 medium. Cells were carefully washed once with phosphate-buffered saline (PBS) and cultured in  
422 2.5 mL of conditioned medium (retained old medium and fresh medium in a ratio of 1:2). In studies  
423 of kinetics of viral progeny release, 200  $\mu$ L of supernatant medium were collected at the appropriate  
424 time points for viral titration on Vero cells as above, and an equal volume of fresh medium was  
425 replaced in the culture tubes. To evaluate the viral RNA yield, cells were harvested, centrifuged at  
426  $7,168 \times g$  for 10 min and washed once with PBS before lysis.

427 Infections of tick cells with UV-inactivated HAZV were performed using a viral stock inactivated  
428 as previously described (42). Briefly, an aliquot of 1 ml virus stock in a well of a 6-well plate was  
429 irradiated with UV (UV Mineral light lamp, model UVG-54, 254 nm, UVP, Upland, CA) at a  
430 distance of 17 mm for 1 min.

431

432 **Immunostaining.** Tick cells were collected and centrifuged at  $206 \times g$  for 7 min and washed once  
433 with PBS, and finally resuspended in PBS. Cells ( $0.6 \times 10^6$  in 200  $\mu$ L) were applied to cleaned  
434 microscope slides using a Shandon III cytocentrifuge (3 min at 1000 rpm). After centrifugation,

435 cells were fixed in 70% ethanol at 4 °C for 30 min and an immunofluorescence assay was  
436 performed. Nonspecific sites were blocked using 2.5% bovine serum albumin (BSA, Sigma) in PBS  
437 and incubation for 1 h at room temperature. Subsequently, slides were incubated for 1.5 h at 37 °C  
438 with the above-mentioned anti-N antibody diluted 1:200 in PBS with 2.5% BSA and 0.1% Tween  
439 20. After this incubation, slides were washed with PBS and incubated for 1 h at 37 °C in the dark  
440 with Alexa Fluor™ 488 goat anti-rabbit IgG (Invitrogen) diluted 1:1000 in PBS with 2.5% BSA  
441 and 0.1% Tween 20, and nuclei were stained with a 1:1000 dilution of 5mM DRAQ5 solution  
442 (Thermo-Fisher Scientific).

443 After this last incubation, infected and mock-infected control cells were examined under a Nikon  
444 A1RSi Laser Scanning inverted confocal microscope equipped with NIS-Elements Advanced  
445 Research software (Nikon Instruments Inc., Tokyo, Japan) and blue (488 nm) and green (561 nm)  
446 lasers.

447

448 **Western blot analysis.** Tick cell cultures were harvested and washed in PBS by centrifugation at  
449  $335 \times g$  for 7 min at 4 °C and then lysed in 100  $\mu$ l of 1X radioimmunoprecipitation assay (RIPA)  
450 buffer (PBS containing 1 % Nonidet P-40, 0.5 % deoxycholate and 0.05 % SDS) in the presence of  
451 protease inhibitors (0.1 mM N $\alpha$ -p-tosyl-L-lysine chloromethyl ketone, 0.1 mM tosylsulfonyl  
452 phenylalanyl chloromethyl ketone, Complete Protease Inhibitor Cocktail Tablets, Roche). Samples  
453 were boiled for 5 min at 100 °C and directly resolved by sodium dodecyl sulfate-polyacrylamide gel  
454 electrophoresis (4.5% stacking gel and 10% resolving gel). Proteins were electroblotted onto a  
455 Hybond ECL nitrocellulose membrane (GE Healthcare Life Sciences). The N protein was detected  
456 by employing the above-mentioned rabbit polyclonal anti-CCHFV nucleoprotein antibody followed  
457 by anti-rabbit HRP-conjugated IgG. The loading control was evaluated using a rabbit polyclonal  
458 anti-calnexin antibody (In-house, Agrisera). Blots were developed with enhanced  
459 chemiluminescence reagents (Amersham Pharmacia) (43). Western blot quantification was

460 performed using the software provided with the Alliance Q9 advanced chemiluminescence imager  
461 (Uvitec; Cleaver Scientific).

462

463 **Drug treatments.** AZT (Sigma) was dissolved in DMSO to a final concentration of 5M while  
464 ribavirin (Sigma) was dissolved in ultrapure H<sub>2</sub>O (MilliQ, Merck) to a final concentration of  
465 100mM. Aliquots were stored at -20 °C. For treatment of cell cultures, half the volume of culture  
466 medium was removed and replaced with fresh medium containing the drug. Cells were incubated  
467 until the indicated time points. Then, cells were detached by pipetting, centrifuged at 2,205 × g for  
468 10 min and washed once with PBS. Cell pellets were then processed for DNA or RNA extraction.

469

470 **Nucleic acid isolation and qRT-PCR analysis.** DNA and RNA were extracted using a DNeasy  
471 Blood & Tissue Kit and a RNeasy Mini Kit (Qiagen) respectively, according to the manufacturer's  
472 instructions. HAZV RNA was amplified using the Superscript III Platinum One-step kit  
473 (Invitrogen) following the standard PCR conditions for TaqMan probes using primers and probe  
474 targeting the S segment (21). Kinetics of intracellular viral RNA replication were evaluated using  
475 the  $\Delta\Delta C_t$  method for the relative quantification of RNA (set to 1 at day 0) using the putative  
476 translation elongation factor EF-1 alpha/Tu endogenous gene of *H. anatolicum* tick cells to  
477 normalize the viral RNA (9, 44).

478 The yield of intracellular HAZV RNA in the ribavirin and AZT experiments was evaluated using a  
479 standard curve generated from six serial dilutions (from  $5 \times 10^6$  to 50 copies) of a control plasmid  
480 containing the region amplified by the primers. The HAZV RNA copy number of the samples was  
481 calculated automatically with the software of the ABI 7900HT Sequence Detection Systems  
482 (Thermo Fisher Scientific) and then expressed as numbers of viral RNA copies per 0.2  $\mu$ g of total  
483 RNA.

484

485 **Detection of vDNAs**

486 PCRs were performed on total DNA extracted from infected HAE/CTVM8 cells with nine pairs of  
487 primers mapping within the S segment of the HAZV genome (GenBank: KP406725.1) and the  
488 CCHFV genome (GenBank: U88410.1). Primers used in this study were designed using the  
489 program “Primer3” available online (<http://bioinfo.ut.ee/primer3-0.4.0/>). The primer sequences are  
490 available on request.

491 Each PCR reaction mixture contained 5  $\mu$ L of 10 $\times$  PCR buffer with 15 mM MgCl<sub>2</sub>, 1  $\mu$ L of 0.625  
492 mM dNTPs mix, 2  $\mu$ L of each primer (10  $\mu$ M), 0.5  $\mu$ L of TaqGold, 50 ng of DNA and PCR grade  
493 water up to the final reaction volume of 50  $\mu$ L (all reagents were purchased from Thermo  
494 Scientific). Cycling conditions were: 1 cycle of 10 min at 95  $^{\circ}$ C; 40 cycles of 15 s at 95  $^{\circ}$ C, 30 s at  
495 60  $^{\circ}$ C and 45 s at 72  $^{\circ}$ C; 5 min at 72  $^{\circ}$ C. Twenty microliters of each PCR product were loaded onto  
496 a 2% (w/v) agarose gel containing the GelRed<sup>®</sup> Nucleic Acid Gel Stain (Biotium).

497

#### 498 ***In vitro* reverse transcriptase assay**

499 To extract proteins, cells were lysed in CHAPS lysis buffer (10 mM Tris-HCl pH 7.5, 400 mM  
500 NaCl, 0.7 mM MnCl<sub>2</sub>, 1mM MgCl<sub>2</sub>, 1mM EGTA, 0.5% CHAPS, 10% glycerol, freshly  
501 supplemented with complete EDTA-free protease inhibitors cocktail [Roche] and 1mM DTT). After  
502 incubation at 4  $^{\circ}$ C for 10 min, cell debris was removed by centrifugation at 16,900  $\times$  g for 10 min at  
503 4  $^{\circ}$ C. Supernatants were transferred to clean tubes. Total protein concentration was determined  
504 using a Micro BCA protein Assay Kit (Thermo Scientific) following the manufacturer’s instructions.  
505 Reverse transcriptase assays were carried out for 15 min at 25  $^{\circ}$ C in a total reaction volume of 50  $\mu$ L  
506 containing 4  $\mu$ g of protein sample, 320 ng of PAGE-purified oligo(dT)<sub>18</sub>, 500 ng of poly(rA), and 1  
507  $\mu$ L of 84 Ci/mmol 3H-dTTP in 50 mM Tris-HCl (pH 7.5), 50 mM KCl, 5mM MgCl<sub>2</sub>, 5mM DTT  
508 and 0.1% Triton X-100. After this, the entire 50  $\mu$ L of each reaction was spotted on an ion paper  
509 (Amersham Hybond-N+, GE Healthcare) that retains incorporated nucleotides but not free dNTPs.  
510 Papers were washed 3 times (10 min for each wash) with saline-sodium citrate buffer (0.3 M NaCl,

511 0.03 M sodium citrate pH 7.2) and immersed in 4 mL of liquid scintillation cocktail Ultima Gold™  
512 (PerkinElmer). Radioactivity was measured using a Scintillator (TRI-carb 2819 TR, Perkin Elmer).

513

514 **Statistical analyses.** Graphs and statistical comparisons, applying Student's t-test, were performed  
515 with the GraphPad Prism 8 software (21). Data subjected to statistical analyses have been replicated  
516 in at least 3 independent experiments. Differences were considered to be statistically significant at p  
517 < 0.05.

518

## 519 **ACKNOWLEDGMENTS**

520 The tick cell lines HAE/CTVM8 and HAE/CTVM9 were provided by the Tick Cell Biobank.

521 This work was supported by University of Padova grants (DOR 2017-2019 and PRID 2017) to CS,

522 ArboNET (2015–01885), Swedish Research Council grants (2017–03126) to AM, and United

523 Kingdom Biotechnology and Biological Sciences Research Council grants BB/N023889/2 and

524 BB/P024270/1 to LB-S. M.V.S was supported by a fellowship of the PhD School in Molecular

525 Medicine, University of Padova.

526

## 527 **REFERENCES**

528 1. Spengler JR, Bente DA, Bray M, Burt F, Hewson R, Korukluoglu G, Mirazimi A, Weber F,

529 Papa A. 2018. Second International Conference on Crimean-Congo Hemorrhagic Fever.

530 *Antiviral Res* 150:137–147.

531 2. Papa A, Mirazimi A, Köksal I, Estrada-Pena A, Feldmann H. 2015. Recent advances in

532 research on Crimean-Congo hemorrhagic fever. *J Clin Virol* 64:137–143.

533 3. Mehand MS, Al-Shorbaji F, Millett P, Murgue B. 2018. The WHO R&D Blueprint: 2018

534 review of emerging infectious diseases requiring urgent research and development efforts.

535 *Antiviral Res* 159:63–67.

536 4. Maes P, Alkhovsky S V., Bào Y, Beer M, Birkhead M, Briese T, Buchmeier MJ, Calisher

537 CH, Charrel RN, Choi IR, Clegg CS, de la Torre JC, Delwart E, DeRisi JL, Di Bello PL, Di  
538 Serio F, Digiario M, Dolja V V., Drosten C, Druciarek TZ, Du J, Ebihara H, Elbeaino T,  
539 Gergerich RC, Gillis AN, Gonzalez JPJ, Haenni AL, Hepojoki J, Hetzel U, Hồ T, Hóng N,  
540 Jain RK, Jansen van Vuren P, Jin Q, Jonson MG, Junglen S, Keller KE, Kemp A, Kipar A,  
541 Kondov NO, Koonin E V., Kormelink R, Korzyukov Y, Krupovic M, Lambert AJ, Laney  
542 AG, LeBreton M, Lukashevich IS, Marklewitz M, Markotter W, Martelli GP, Martin RR,  
543 Mielke-Ehret N, Mühlbach HP, Navarro B, Ng TFF, Nunes MRT, Palacios G, Pawęska JT,  
544 Peters CJ, Plyusnin A, Radoshitzky SR, Romanowski V, Salmenperä P, Salvato MS,  
545 Sanfaçon H, Sasaya T, Schmaljohn C, Schneider BS, Shirako Y, Siddell S, Sironen TA,  
546 Stenglein MD, Storm N, Sudini H, Tesh RB, Tzanetakis IE, Uppala M, Vapalahti O,  
547 Vasilakis N, Walker PJ, Wáng G, Wáng L, Wáng Y, Wèi T, Wiley MR, Wolf YI, Wolfe ND,  
548 Wú Z, Xú W, Yang L, Yāng Z, Yeh SD, Zhāng YZ, Zhèng Y, Zhou X, Zhū C, Zirkel F,  
549 Kuhn JH. 2018. Taxonomy of the family Arenaviridae and the order Bunyavirales: update  
550 2018. *Arch Virol* 163:2295–2310.

551 5. Akıncı E, Bodur H, Leblebicioglu H. 2013. Pathogenesis of Crimean-Congo Hemorrhagic  
552 Fever. *Vector-Borne Zoonotic Dis* 13:429–437.

553 6. Bente DA, Forrester NL, Watts DM, McAuley AJ, Whitehouse CA, Bray M. 2013. Crimean-  
554 Congo hemorrhagic fever: history, epidemiology, pathogenesis, clinical syndrome and  
555 genetic diversity. *Antiviral Res* 100:159–189.

556 7. Xia H, Beck AS, Gargili A, Forrester N, Barrett ADT, Bente DA. 2016. Transstadial  
557 Transmission and Long-term Association of Crimean-Congo Hemorrhagic Fever Virus in  
558 Ticks Shapes Genome Plasticity. *Sci Rep* 6:35819.

559 8. Thangamani S, Bente D. 2014. Establishing protocols for tick containment at Biosafety Level  
560 4. *Pathog Dis* 71:282–285.

561 9. Salata C, Monteil V, Karlberg H, Celestino M, Devignot S, Leijon M, Bell-Sakyi L,  
562 Bergeron É, Weber F, Mirazimi A. 2018. The DEVD motif of Crimean-Congo hemorrhagic



- 563 fever virus nucleoprotein is essential for viral replication in tick cells. *Emerg Microbes Infect*  
564 7:190.
- 565 10. Salata C, Moutailler S, Attoui H, Zweygarth E, Decker L, Bell-Sakyi L. 2021. How relevant  
566 are in vitro culture models for study of tick-pathogen interactions? *Pathog Glob Health*  
567 <https://doi.org/10.1080/20477724.2021.1944539>.
- 568 11. Begum F, Wisseman CL, Casals J. 1970. Tick-borne viruses of West Pakistan. II. Hazara  
569 virus, a new agent isolated from *Ixodes redikorzevi* ticks from the Kaghan Valley, W.  
570 Pakistan. *Am J Epidemiol* 92:192–194.
- 571 12. Kuhn JH, Wiley MR, Rodriguez SE, Bào Y, Prieto K, Travassos da Rosa APA, Guzman H,  
572 Savji N, Ladner JT, Tesh RB, Wada J, Jahrling PB, Bente DA, Palacios G. 2016. Genomic  
573 characterization of the genus nairovirus (Family Bunyaviridae). *Viruses* 8(6):164.
- 574 13. Kalkan-Yazıcı M, Karaaslan E, Çetin NS, Hasanoğlu S, Güney F, Zeybek Ü, Doymaz MZ.  
575 2021. Cross-Reactive Anti-Nucleocapsid Protein Immunity against Crimean-Congo  
576 Hemorrhagic Fever Virus and Hazara Virus in Multiple Species. *J Virol* 95(7):e02156-20.
- 577 14. Fuller J, Surtees RA, Shaw AB, Álvarez-Rodríguez B, Slack GS, Bell-Sakyi L, Mankouri J,  
578 Edwards TA, Hewson R, Barr JN. 2019. Hazara nairovirus elicits differential induction of  
579 apoptosis and nucleocapsid protein cleavage in mammalian and tick cells. *J Gen Virol*  
580 100:392–402.
- 581 15. Fuller J, Surtees RA, Slack GS, Mankouri J, Hewson R, Barr JN. 2019. Rescue of Infectious  
582 Recombinant Hazara Nairovirus from cDNA Reveals the Nucleocapsid Protein DQVD  
583 Caspase Cleavage Motif Performs an Essential Role other than Cleavage. *J Virol*  
584 93(15):e00616-19.
- 585 16. Matsumoto Y, Nouchi T, Ohta K, Nishio M. 2019. Regulation of Hazara virus growth  
586 through apoptosis inhibition by viral nucleoprotein. *Arch Virol* 164:1597–1607.
- 587 17. Surtees R, Dowall SD, Shaw A, Armstrong S, Hewson R, Carroll MW, Mankouri J, Edwards  
588 TA, Hiscox JA, Barr JN. 2016. Heat Shock Protein 70 Family Members Interact with

- 589 Crimean-Congo Hemorrhagic Fever Virus and Hazara Virus Nucleocapsid Proteins and  
590 Perform a Functional Role in the Nairovirus Replication Cycle. *J Virol* 90:9305–9316.
- 591 18. Karlberg H, Tan Y-J, Mirazimi A. 2011. Induction of Caspase Activation and Cleavage of  
592 the Viral Nucleocapsid Protein in Different Cell Types during Crimean-Congo Hemorrhagic  
593 Fever Virus Infection. *J Biol Chem* 286:3227–3234.
- 594 19. Karlberg H, Tan Y-J, Mirazimi A. 2015. Crimean-Congo haemorrhagic fever replication  
595 interplays with regulation mechanisms of apoptosis. *J Gen Virol* 96:538–546.
- 596 20. Carter SD, Surtees R, Walter CT, Ariza A, Bergeron E, Nichol ST, Hiscox JA, Edwards TA,  
597 Barr JN. 2012. Structure, Function, and Evolution of the Crimean-Congo Hemorrhagic Fever  
598 Virus Nucleocapsid Protein. *J Virol* 86:10914–10923.
- 599 21. Monteil V, Salata C, Appelberg S, Mirazimi A. 2020. Hazara virus and Crimean-Congo  
600 Hemorrhagic Fever Virus show a different pattern of entry in fully-polarized Caco-2 cell line.  
601 *PLoS Negl Trop Dis* 14:e0008863.
- 602 22. Dowall SD, Findlay-Wilson S, Rayner E, Pearson G, Pickersgill J, Rule A, Merredew N,  
603 Smith H, Chamberlain J, Hewson R. 2012. Hazara virus infection is lethal for adult type I  
604 interferon receptor-knockout mice and may act as a surrogate for infection with the human-  
605 pathogenic Crimean-Congo hemorrhagic fever virus. *J Gen Virol* 93:560–564.
- 606 23. Bell-Sakyi L. 1991. Continuous cell lines from the tick *Hyalomma anatolicum anatolicum*. *J*  
607 *Parasitol* 77:1006–1008.
- 608 24. Goic B, Vodovar N, Mondotte JA, Monot C, Frangeul L, Blanc H, Gausson V, Vera-Otarola  
609 J, Cristofari G, Saleh MC. 2013. RNA-mediated interference and reverse transcription  
610 control the persistence of RNA viruses in the insect model *Drosophila*. *Nat Immunol* 14:396–  
611 403.
- 612 25. Goic B, Stapleford KA, Frangeul L, Doucet AJ, Gausson V, Blanc H, Schemmel-Jofre N,  
613 Cristofari G, Lambrechts L, Vignuzzi M, Saleh MC. 2016. Virus-derived DNA drives  
614 mosquito vector tolerance to arboviral infection. *Nat Commun* 7:1–10.

- 615 26. Han Y, Wu Q, Ding SW. 2018. Templating Antiviral RNAi in Insects. *Cell Host Microbe*  
616 23(3):290-292.
- 617 27. Bell-Sakyi L, Kohl A, Bente DA, Fazakerley JK. 2012. Tick cell lines for study of Crimean-  
618 Congo hemorrhagic fever virus and other arboviruses. *Vector Borne Zoonotic Dis* 12:769–  
619 781.
- 620 28. Logan TM, Linthicum KJ, Bailey CL, Watts DM, Dohm DJ, Moulton JR. 1990. Replication  
621 of Crimean-Congo Hemorrhagic Fever Virus in Four Species of Ixodid Ticks (Acari)  
622 Infected Experimentally. *J Med Entomol* 27:537–542.
- 623 29. Honig JE, Osborne JC, Nichol ST. 2004. The high genetic variation of viruses of the genus  
624 Nairovirus reflects the diversity of their predominant tick hosts. *Virology* 318:10–16.
- 625 30. Růžek D, Bell-Sakyi L, Kopecký J, Grubhoffer L. 2008. Growth of tick-borne encephalitis  
626 virus (European subtype) in cell lines from vector and non-vector ticks. *Virus Res* 137:142–  
627 146.
- 628 31. Kholodilov IS, Litov AG, Klimentov AS, Belova OA, Polienko AE, Nikitin NA, Shchetinin  
629 AM, Ivannikova AY, Bell-Sakyi L, Yakovlev AS, Bugmyrin S V., Bespyatova LA, Gmyl L  
630 V., Luchinina S V., Gmyl AP, Gushchin VA, Karganova GG. 2020. Isolation and  
631 Characterisation of Alongshan Virus in Russia. *Viruses* 12:362.
- 632 32. Belova OA, Litov AG, Kholodilov IS, Kozlovskaya LI, Bell-Sakyi L, Romanova LI,  
633 Karganova GG. 2017. Properties of the tick-borne encephalitis virus population during  
634 persistent infection of ixodid ticks and tick cell lines. *Ticks Tick Borne Dis* 8:895–906.
- 635 33. Bell-Sakyi L, Attoui H. 2016. Article Commentary: Virus Discovery Using Tick Cell Lines.  
636 *Evol Bioinforma* 12s2:EBO.S39675.
- 637 34. Nag DK, Brecher M, Kramer LD. 2016. DNA forms of arboviral RNA genomes are  
638 generated following infection in mosquito cell cultures. *Virology* 498:164–171.
- 639 35. Olson KE, Bonizzoni M. 2017. Nonretroviral integrated RNA viruses in arthropod vectors:  
640 an occasional event or something more? *Curr Opin Insect Sci* 22:45-53.

- 641 36. Poirier EZ, Goic B, Tomé-Poderti L, Frangeul L, Boussier J, Gausson V, Blanc H, Vallet T,  
642 Loyd H, Levi LI, Lanciano S, Baron C, Merklings SH, Lambrechts L, Mirouze M, Carpenter  
643 S, Vignuzzi M, Saleh MC. 2018. Dicer-2-Dependent Generation of Viral DNA from  
644 Defective Genomes of RNA Viruses Modulates Antiviral Immunity in Insects. *Cell Host*  
645 *Microbe* 23:353-365.e8.
- 646 37. Houé V, Gabiane G, Dauga C, Suez M, Madec Y, Mousson L, Marconcini M, Yen PS, de  
647 Lamballerie X, Bonizzoni M, Failloux AB. 2019. Evolution and biological significance of  
648 flaviviral elements in the genome of the arboviral vector *Aedes albopictus*. *Emerg Microbes*  
649 *Infect* 8:1265–1279.
- 650 38. Houé V, Bonizzoni M, Failloux AB. 2019. Endogenous non-retroviral elements in genomes  
651 of *Aedes* mosquitoes and vector competence. *Emerg Microbes Infect* 8(1):542-555.
- 652 39. Forth JH, Forth LF, Lycett S, Bell-Sakyi L, Keil GM, Blome S, Calvignac-Spencer S,  
653 Wissgott A, Krause J, Höper D, Kampen H, Beer M. 2020. Identification of African swine  
654 fever virus-like elements in the soft tick genome provides insights into the virus' evolution.  
655 *BMC Biol* 18(1):136.
- 656 40. Russo AG, Kelly AG, Enosi Tuipulotu D, Tanaka MM, White PA. 2019. Novel insights into  
657 endogenous RNA viral elements in *Ixodes scapularis* and other arbovirus vector genomes.  
658 *Virus Evol* 5(1):vez010.
- 659 41. Nag DK, Kramer LD. 2017. Patchy DNA forms of the Zika virus RNA genome are generated  
660 following infection in mosquito cell cultures and in mosquitoes. *J Gen Virol* 98:2731–2737.
- 661 42. Andersson I, Karlberg H, Mousavi-Jazi M, Martínez-Sobrido L, Weber F, Mirazimi A. 2008.  
662 Crimean-Congo hemorrhagic fever virus delays activation of the innate immune response. *J*  
663 *Med Virol* 80:1397–1404.
- 664 43. Calistri A, Munegato D, Toffoletto M, Celestino M, Franchin E, Comin A, Sartori E, Salata  
665 C, Parolin C, Palù G. 2015. Functional Interaction Between the ESCRT-I Component  
666 TSG101 and the HSV-1 Tegument Ubiquitin Specific Protease. *J Cell Physiol* 230:1794–

667 1806.

668 44. Salata C, Monteil V, Leijon M, Bell-Sakyi L, Mirazimi A. 2020. Identification and validation  
669 of internal reference genes for real-time quantitative polymerase chain reaction-based studies  
670 in *Hyalomma anatolicum* ticks. *Ticks Tick Borne Dis* 14(11):e0008863.

671

672

673

674

675

676

677

678

679